Astron. Astrophys. 343, L65–L69 (1999)

ASTRONOMY AND ASTROPHYSICS

LETTER

Letter to the Editor

An ultra-deep ISOCAM observation through a cluster-lens⋆

B. Altieri[1], L. Metcalfe[1], J.P. Kneib[2], B. McBreen[3], H. Aussel[4], A. Biviano[5], M. Delaney[3], D. Elbaz[4], K. Leech[1], L. Lémonon[4], K. Okumura[6], R. Pelló[2], and B. Schulz[1]

[1] ISO Data Centre, Astrophysics Division, Space Science Department of ESA, Villafranca del Castillo, P.O. Box 50727, E-28080 Madrid, Spain
[2] Observatoire Midi-Pyréneés, 14 Av. E. Belin, F-31400 Toulouse, France
[3] Physics Department, University College Dublin, Stillorgan Rd., Dublin 4, Ireland
[4] DSM/DAPNIA/SAp, CEA-Saclay, F-91191 Gif-sur-Yvette Cedex, France
[5] Osservatorio Astronomico di Trieste, via G.B. Tiepolo 11, I-34131 Trieste, Italy
[6] Institut d'Astrophysique Spatiale, Bât. 121, Université Paris-Sud, F-91405 Orsay, France

Received 30 October 1998 / Accepted 3 February 1999

Abstract. We present results of ultra-deep ISOCAM observations through a cluster-lens at 7μm and 15μm with the Infrared Space Observatory (ISO) satellite. These observations reveal a large number of luminous Mid-Infrared (MIR) sources. Cross-identification in the optical and Near-Infrared (NIR) wavebands shows that about half of the 7 μm sources are cluster galaxies. The other 7 μm and almost all 15 μm sources are identified as lensed distant galaxies. Thanks to the gravitational amplification they constitute the faintest sources detected in the MIR, allowing us to extend the number counts in both the 7 and 15 μm bands. In particular, we find that the 15 μm counts have a steep slope $\alpha_{15\mu\mathrm{m}} = -1.5 \pm 0.3$ and are large, with $\mathrm{N}_{15\mu\mathrm{m}}(> 30\mu\mathrm{Jy}) = 13 \pm 5$ arcmin^{-2}. These numbers rule out non-evolutionary models and favour very strong evolution. Down to our counts limit, we found that the resolved 7 μm and 15 μm background radiation intensities are respectively (1.7±0.5)×10^{-9} and (3.3±1.3)×10^{-9} W m^{-2} sr^{-1}.

Key words: galaxies: abundances – galaxies: clusters: general – galaxies: evolution – cosmology: gravitational lensing – infrared: galaxies

1. Introduction

Great progress in the understanding of physical properties of galaxies has been achieved with Mid-Infrared (MIR) and Far Infrared (FIR) observations using the ISO satellite (Kessler et al. 1996) and its ISOCAM camera (Cesarsky et al. 1996).

Deep optical surveys revealed a new population of distant sources at high-redshift ($z > 2.5$), either using 'drop-out' techniques (Steidel et al. 1996), or 'photometric redshift' (e.g. Lanzetta et al. 1996). Yet optical surveys may miss a whole class of high-redshift dust-enshrouded galaxies (Blain & Longair 1993). Indeed, galaxy formation models (e.g. Arimoto & Yoshi 1987, Guiderdoni et al. 1997) predict that galaxies in their forming phase are heavily obscured by abundant gas and dust inside the system. These issues have motivated very deep ISOCAM observations of blank fields (Rowan-Robinson et al. 1997; Taniguchi et al. 1997), as well as Sub-millimeter observations (Smail et al. 1997; Barger et al. 1998; Hughes et al. 1998).

The ISOCAM-HDF observations showed that 15μm results rule out a no-evolution model (Oliver et al. 1997). Analysing galaxy counts over a wide range of sensitivity, Elbaz et al. (1998) noted a change of slope in the counts observed at the mJy-level. This variation requires stronger star-formation activity at moderate redshifts.

We report here very deep ISOCAM observations conducted through a gravitationally lensing cluster of galaxies as part of a large programme using gravitational lensing to achieve fainter detection thresholds in a given observation time. The full programme is reported elsewhere (Metcalfe et al. 1999a and b). By pushing ISOCAM to its ultimate limits with the help of gravitational lensing, we achieved ultra-deep observations through the core of probably the best studied lensing cluster: Abell 2390 ($z = 0.23$), to obtain a magnified view of the background sky. This both increases the sensitivity of our MIR maps and reduces the effects of source confusion.

2. Observations and data reduction

2.1. Observations

The observations reported here were allocated one full ISO revolution (science window of 16 hours) of ESA guaranteed time. We used the best observational strategy for detection of faint sources, based upon in-flight experience (Altieri et al. 1998). In particular, the field was observed redundantly in 4 consec-

Send offprint requests to: B. Altieri (baltieri@iso.vilspa.esa.es)

⋆ Based on observations with ISO, an ESA project with instruments funded by ESA Member States (especially the PI countries: France, Germany, the Netherlands and the United Kingdom) with the participation of ISAS and NASA

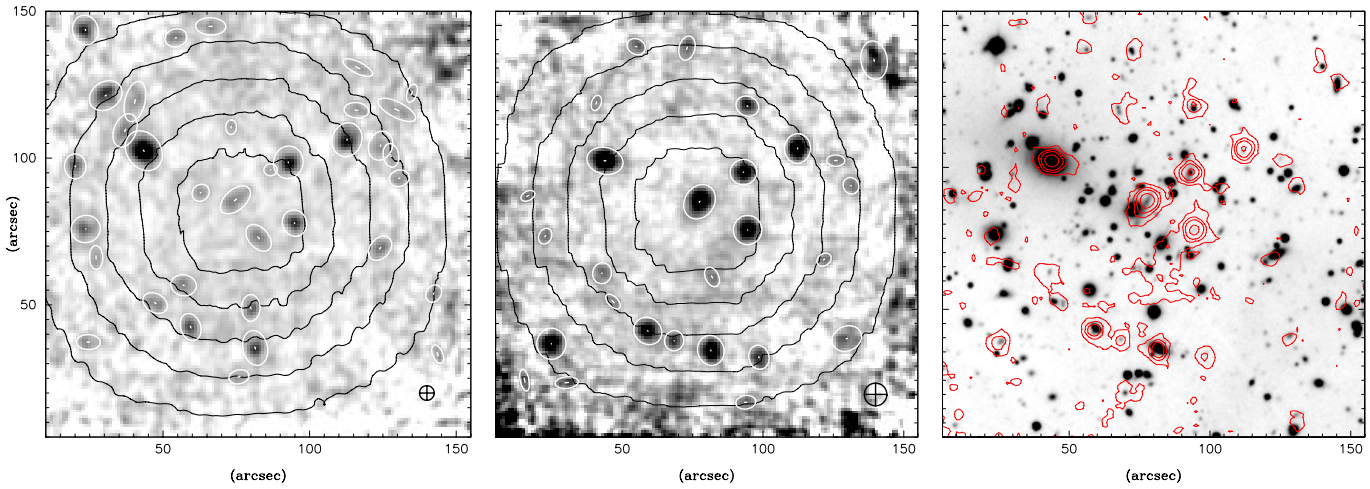

Fig. 1. MIR image of the A2390 cluster: (*left*) LW2 image, (*middle*) LW3 image. For these 2 images, the beam size (defined as 80% of encircled energy) is indicated in the lower-righthand corner; objects detected with the SExtractor software are indicated by ellipses; contours show the iso-exposure-time of 5ks, 10ks, 15ks, 20ks and 25ks. (*right*) LW3 significance image (weighting the image by the square root of the effective integration time per pixel) overlaid on a ground-based Gunn R image

utive revolutions in 4 blocks of 4 hours. The allocated time was equally divided between the 2 broad-band ISOCAM filters LW2 (5-8.5μm), with reference wavelength 6.75μm, and LW3 (12-18μm), with reference wavelength 15 μm.

We rastered the 32×32-ISOCAM detector array in microscanning mode. The pixel-field-of-view (PFOV) of 3″ per pixel-field-of-view (PFOV) was chosen to obtain high spatial resolution, giving a good sampling of the PSF, crucial for source cross-identification. The raster step size was 7″ (2.33 PFOV), the minimum value to step out of the PSF FWHM in two consecutive pointings. The size of rasters was 10×10, so that, in the central part of each single raster, 100 different detector pixels sampled each sky pixel. Such redundancy was a key factor in ISOCAM deep observations. The final maps cover a field size of 2.6′×2.6′. These new observations supercede in area and depth the previous ISOCAM observations of this cluster (Lémonon et al. 1998).

2.2. Data reduction and calibration

The Abell 2390 raw data from this programme and the Lémonon et al. (1998) data were processed together following the steps:

i) Dark subtraction using a time-dependent dark correction (Biviano et al. 1998).
ii) Deglitching, flat-fielding and sky subtraction of each raster was performed using the PRETI Multi-resolution Median Transform techniques adapted for ISOCAM data analysis (Starck et al. 1997), a multi-scale analysis that decomposes temporally the different parts of the signals.
iii) Field distortion correction (Aussel et al. 1998) for sky projection, with a final pixel size of 1″.
iv) The 5 rasters were then stacked together using the drizzling technique described by Fruchter & Hook 1998. The rasters were aligned using the centroids of the 4 to 5 brightest sources in each waveband.

The calibration into μJy was done using the refined in-flight calibration values from Blommaert et al. (1998).

We took into account the transient behaviour of the ISOCAM pixel signals, which do not stabilize at faint fluxes, but respond to a change in illumination level with transient drifts that depend both on the background level and the source intensity. We calibrated the impact of these responsive transients for our observational parameters by applying the IAS transient correction model of Abergel et al. (1996) to our data. This showed that our LW2 and LW3 responsivities were 60% and 80% of nominal, respectively.

The central parts of the stacked 7 and 15 μm images are shown respectively in Fig. 1.

3. Analysis and results

3.1. Detection and photometry

Source catalogs from our field in LW2 and LW3 were constructed using the SExtractor package (Bertin & Arnouts, 1996). The detection algorithm searches for 15 contiguous pixels, each having a surface brightness exceeding a threshold (chosen as 1.5 σ of the sky noise), after subtracting a smooth background signal and convolving the image with a gaussian filter of the same width as the 7 and 15 μm image PSF. We performed 7″ aperture photometry. Aussel et al. (1998) showed that aperture photometry is very linear above 100 μJy, though at the faintest fluxes the remnants of cosmic rays pollute the sources with a positive bias. The photometry was corrected for loss of flux in the PSF wings, by using measurements of calibration stars under similar conditions (microscanning & rastering): 60% of the signal is found within a 7″ diameter at 7 μm and 48% at 15 μm.

To assess the contribution of noise to our catalogs we ran the detection algorithm on the negative fluctuations in the maps, concluding that we have no false detections above 60 μJy in the central 2.25′×2.25′ area of the maps in both filter bands.

Table 1. MIR source counts in the image plane, N: number of detected sources, N_{neg}: number of detected sources on the inverted image

λ (μm)	Threshold μJy/beam (3σ)	N	N_{neg}	$S_{80\%}$ μJy	$S_{50\%}$ μJy
7	25	31	0	70	40
15	40	34	0	100	60

Finally, to determine the completeness of the sample we added a template faint source (scaled-down version of a calibration star) to the maps repeatedly at different positions in the map and estimated the efficiency of detecting this source as a function of its flux density. This provided a reliable estimate of the visibility of a faint compact source in the maps. The estimated 80% and 50% completeness limits of the catalogs derived from these simulations are listed in Table 1. These numbers refer to apparent source brightness before lensing correction. They are similar to the deepest observations published to date at 7 μm on the Lockman Hole (Taniguchi et al. (1997) report faintest detections around 30μJy) and at 15 μm on the HDF (where the faintest sources are around 50 μJy). However, thanks to the gravitational magnification of a factor $\sim$2 to 10, the sources are intrisically the faintest MIR sources detected to date.

3.2. Cluster contamination

Thanks to our high-resolution images we have been able to unambiguously identify more than 90% of the sources with counterparts in deep NIR and optical (HST/WFPC2 and ground-based) images. The relative astrometric accuracy is found to be better than 1″ in both filters. In only a few cases we do suspect that two sources are blended. There is one obvious case in the 7 μm map, where the *straight arc* (Pelló et al. 1991) is blended with the nearby elliptical galaxy. Unambiguous cross-identification was possible with detections at other wavelengths thanks to a large density of sources and a good sampling of the PSF, see Fig. 1 (right).

At 7 μm 30 sources are detected. 2 stars and 14 easily identified cluster-member galaxies (Pelló et al. 1991, Leborgne et al. 1992, Abraham et al. 1996). The 5-8.5 μm emission of the cluster galaxies corresponds to 4.5-6.9 μm rest-frame emission. For E/S0 galaxies it corresponds mostly to the Rayleigh-Jeans tail of their old stellar population, as in the Virgo cluster (Boselli et al. 1998). Eleven sources are identified as lensed galaxies. These lensed sources are all detected at 15 μm.

At 15 μm, 34 sources are detected in the central $2.25' \times 2.25'$ field. Only three sources are identified as cluster members: the cD galaxy (Lémonon et al. 1998, Edge et al. 1998) and 2 other galaxies. Based upon spectroscopic or photometric redshifts, all the other sources are identified as faint lensed galaxies. All sources for which we have spectroscopic redshifts are background objects. Although we can not rule out some of the other targets being in the cluster, the probability is very small. The detection of almost exclusively background sources in the cluster images demonstrates that at 15 μm the cluster-core becomes transparent, as in Sub-mm bands (Blain et al. 1997). Therefore the key feature is that the cluster-core acts as a natural gravitational telescope amplifying the flux of background sources, typically by a factor of 2.

3.3. Source counts

The number density of sources is high with respect to the size of the FWHM ($\sim$ 6″ diameter at 15 μm). But the PSF is well sampled on the final maps and its shape can be used to separate the sources. With 25 beams per source, confusion should not be too severe. Only two 15 μm sources lie at the location of pairs of suspected high-z galaxies. The occasional blending of the sources has not been taken into account, but the surface area occupied by bright sources is subtracted for the computation of the surface density of the fainter ones (because other faint sources could be hidden by brighter ones). We used the completeness of the detections at 15 μm given in Table 1. This correction is negligible for the 7 μm counts and was not applied.

Due to the non-uniform sensitivity of our maps, because of the combined effects of observation strategy and the lensing, the object density per flux bin was computed using magnification-dependant surface areas derived from the lensing model so dividing the maps into sub-maps. Only the central $2' \times 2'$ area was taken into account for the faintest fluxes.

A detailed lensing model of A2390 has been produced by Kneib et al. (1999). The lensing acts in two ways on the background population of galaxies. It causes:

i) an amplification of the source brightness, typically by a factor of 2, but up to 10 in the higher gain regions.
ii) a surface dilation effect of the area probed, which itself depends on the redshift; the space dilation is stronger towards the centre (core of the cluster) and increases with source-plane redshift.

To estimate these factors we used the spectroscopic redshift for 7 objects (Pelló et al. 1991, Bézecourt & Soucail 1997), and for the rest we use the best redshift estimate obtained with photometric redshift techniques (Pelló, private communication), and/or lensing inversion techniques (Kneib et al. 1999). By analysing the case with all background galaxies at a mean redshift $\overline{z} = 1.0$, we checked the dependence of the results on redshift uncertainties.

By correcting for the lens magnification and surface dilution effects, contamination by cluster galaxies, and non-uniform sensitivity of our maps, we can derive number counts at 15 μm to compare with *blank* sky counts (e.g. in the Hubble Deep field and Lockman Hole). The 7 μm number counts are more difficult to derive due to the larger contamination by the cluster and because of the small number statistics.

4. Discussion

The source counts, corrected for cluster contamination and lensing effects, in both the LW2 and LW3 bands, are presented in

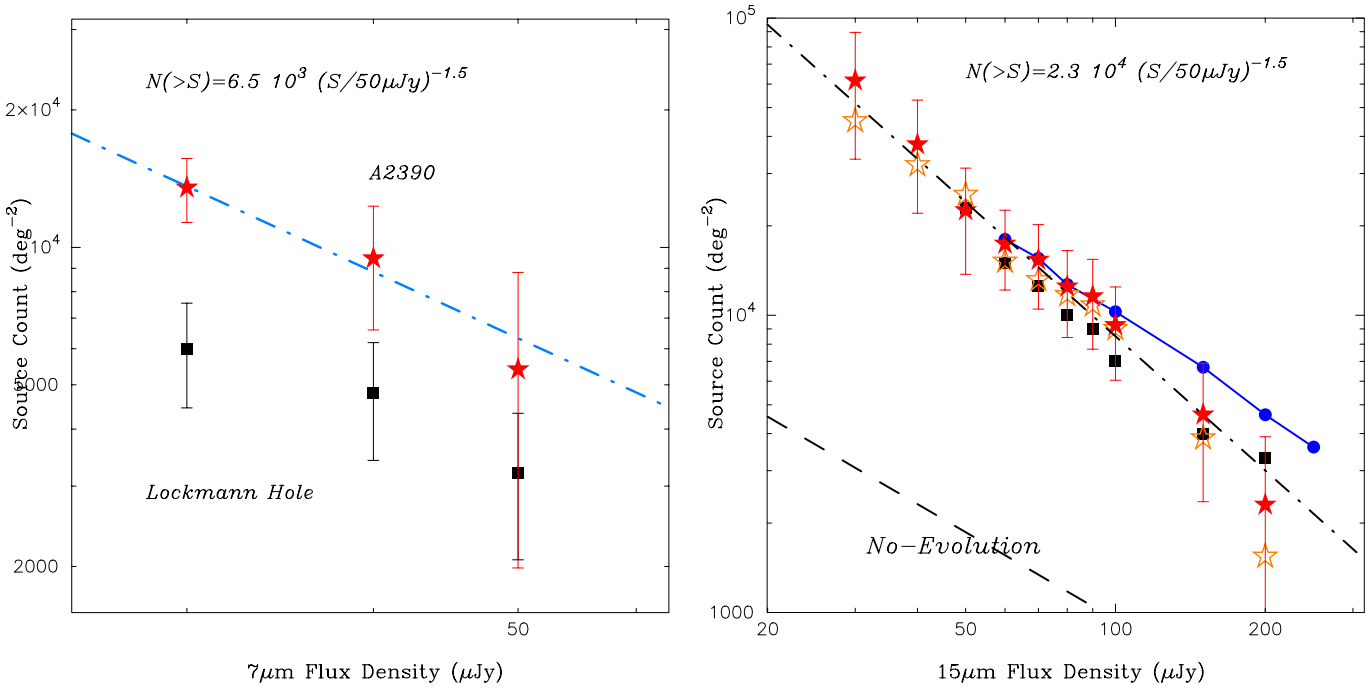

Fig. 2. (*left*) 7 μm lens-corrected counts, of identified field galaxies, (filled stars) compared to the Lockman Hole counts (filled squares) of Taniguchi et al. (1997). (*right*) 15 μm lens-corrected counts corrected for incompleteness, full model (*filled stars*), counts with all sources at z=1 (*open stars*), counts without lensing correction (*filled circles*) down to 60 μJy and compared to the HDF counts (Aussel et al. 1998) (*filled squares*) and the non-evolution model (dashed line) from Franceschini et al. (1994). Error bars include both Poisson and systematic terms.

Fig. 2. At 15 μJy we have used only 5σ sources (i.e. 27 sources above $\sim$60 μJy before lensing amplification correction). According to Hogg & Turner (1998), this is sufficient to avoid the positive flux-estimate Eddington bias which occurs for faint source counts.

At 7 μm, we find a source density greater than that of Taniguchi et al. (1997) by a factor of 2. We suggest that their observations may be incomplete below 50 μJy, whereas our 7 μm map is 80% complete down to 30 μJy in the central $2' \times 2'$ with lensing amplification correction.

At 15 μm the number counts are compatible with the results of Aussel et al. (1998) in the HDF. However, with the help of gravitational lensing we are able to extend the counts in both bands down to 30μJy. Putting all background sources at $z = 1$ only slightly decreases the faintest counts, at the faint end, because a few suspectedly high-z faint sources would be less amplified. This shows the small dependence of our derived counts on the redshift distribution of the sample. The higher lensing-uncorrected counts at the bright end are due to small number statistical bias, where more sources than average appear in the high gain region of the A2390 cluster potential.

We find a total number density $N_7(>30\mu\text{Jy}) = 3.5 \pm 1$ arcmin^{-2} at 7 μm, and $N_{15}(>30\mu\text{Jy}) = 13 \pm 5$ arcmin^{-2} at 15 μm, with a slope $\alpha_{15} = -1.5 \pm 0.3$.

The 15 μm counts show a steadily increasing excess (by more than a factor of 10) with respect to the prediction of a no-evolution model (dashed line, Franceschini et al. 1997). This confirms the steeper count slope below 1 mJy found on the Lockman Hole (Elbaz et al. 1998) and is in good agreement with the ISO HDF counts (Aussel et al. 1998). The counts are a factor 2 to 3 higher than the boundaries of the counts coming from an early analysis of the background fluctuations in the ISOCAM 15 μm map of the HDF (Oliver et al. 1997). The slope stays close to -1.5$\pm$0.3 down to 30 μJy. This source density at faint levels favours evolution models, needed to fit the counts at brighter fluxes (Elbaz et al. 1998), or single-population models (Blain et al. 1998).

Integrating the number counts over our A2390 flux range (30 μJy to 200μJy) and over other ISOCAM deep surveys (Elbaz et al. 1998) up to 50 mJy we find the resolved background to be $(3.3 \pm 0.8) \times 10^{-9}$ and $(1.7 \pm 0.5) \times 10^{-9}$ W m^{-2} sr^{-1} emitted respectively at 15 μm and 7 μm. If we restrict to the very reliable counts, i.e. down to 50 μJy only at 15 μm, we find a conservative background value of $(2.4 \pm 0.8) \times 10^{-9}$ W m^{-2} sr^{-1}. The 15μm lower limit is close to the current upper limits set by the gamma-CMBR photon-photon pair production (Stanev and Franceschini 1997). Note that our 7μm source counts power law slightly underestimates counts at higher fluxes; a slope of -1.3 would be necessary to be compatible with Flores et al. (1999a) counts of $\sim$ 0.45 per arcmin^2 above 150 mJy).

5. Conclusion

In our ultra-deep 15μm survey, deeper by almost a factor of two than other surveys, we do not detect any sign of the flattening of the 15μm counts at the faintest levels, expected from evolutionary models (Franceschini et al. 1994). We derive a resolved MIR cosmic background of 3.3 nW m^{-2} sr^{-1}, with a

median redshift of sources of 0.7 (Metcalfe et al. 1999), similar to $< z >= 0.6$ of ISOCAM sources in the HDF (Aussel et al. 1999). ISO counts demonstrate comparable forms of evolution in the mid-IR to those observed in the CFRS (Flores et al. 1999b), then a larger amount of energy was emitted above z=0.6 than in the local universe.

Deep 15 μm ISOCAM imaging is a good way to select star-forming/AGN galaxies at moderate to high redshifts which are not easy to identify in UV/optical surveys (Ivison et al. 1998, Soucail et al. 1999). A number of these sources are well correlated with faint galaxies in the visible, some of them having very red colours in the NIR. Caution must therefore be employed when inferring global star formation activity based only on UV-continuum or optical luminosities of high-z galaxies. A more detailed analysis of the SED of these MIR detected galaxies will be necessary to unveil the nature of these MIR sources and to give an estimate of their SFR. But our observations confirm already that abundant star formation activity occurs in very dusty environments at $z \sim 1$.

Acknowledgements. JPK acknowledges support from CNRS/INSU. Many thanks to the referee A. Blain and I. Smail for very useful discussions and comments. The ISOCAM data presented in this paper was analysed using "CIA", a joint development by the ESA Astrophysics Division and the ISOCAM Consortium. The ISOCAM Consortium is led by the ISOCAM PI, C. Cesarsky, Direction des Sciences de la Matiere, C.E.A., France.

References

Abergel A., Bernard J.-P., Boulanger F., et al., 1996, A&A, 315, L329
Abraham R, Smecker H., Tammy A. et al., 1996, ApJ, 471, 694
Altieri B., Metcalfe L., Elbaz D. et al., 1998, *Experimental Astronomy*, in press, "ISOCAM Ultimate sensitivity",
Arimoto N., Yoshii Y., 1987, A&A, 173, 23
Aussel H., Cesarsky C.J., Elbaz D., Starck J.-L., 1999, A&A, in press, astro-ph/9810044
Barger A., Cowie L., Sanders D. et al., 1998, Nat., vol. 394
Bertin E. & Arnouts S., 1996. A&A, 177, 393
Bézecourt J. & Soucail G., 1997, A&A, 317, 661-669
Biviano A., Sauvage M., Gallais P., Roman P., Altieri B., 1998, Exp. Astr., in press, "Dark behaviour in ISOCAM LW"
Blain & Longair, 1993, MNRAS, 255, L21
Blain A., 1997, MNRAS, 290, 553
Blain A., Smail I., Ivison R., Kneib J.-P., 1999, MNRAS, in press, astro-ph/9806062
Blommaert J., Metcalfe L., Altieri B., 1998, Exp. Astr., in press, "The ISOCAM responsivity in orbit"
Boselli A., Lequeux J., Sauvage et al., 1998, A&A, 335, 53
Cesarsky C.J. et al., 1996, A&A 315, L32
Edge, A.C, Ivison, R.J., Smail, I., Blain, A.W., Kneib, J.-P., 1999, MNRAS, submitted
Elbaz D., Aussel H., Cesarsky C. J. et al., 1998, Proc. of 34th Liege Int. Astr. Coll. on the NGST, astro-ph/9807209
Flores H., Hammer F., Thuan T.X. et al., 1999a, A&A in press, astro-ph/9811201
Flores H., Hammer F., Thuan T.X., Césarsky C., Désert F.X., et al., 1999b, ApJ in press, astro-ph/9811202
Franceschini A., Mazzei P., De Zotti G., Danese L., 1994, ApJ, 427, 140-154
Fruchter A.& Hook R., 1998, Appl. of Digital Image Proc. XX, ed. A. Tescher, Proc.SPIE. vol.3164 astro-ph/9708242
Guiderdoni, B., Hivon, E., Bouchet, F. R., Maffei, B., 1997, MNRAS, 295, 877.
Hogg D & Turner E., 1998, PASP, 110, 727
Hughes D., Serjeant S., Dunlop J. et al., 1998, Nat., 394, 241
Ivison R., Smail I., Le Borgne J.-F., Blain A., Kneib J.-P., 1998, MNRAS, 298, 583
Kessler M.F. et al., 1996, A&A 315, L27
Kneib et al., 1999, in preparation.
Lanzetta K.M., Webb J., Barcons X., 1996, Nature, 381, 759
Leborgne J.-F., Pelló R., Sanahuja B., 1992, A&AS, 95, 87
Lémonon L., Pierre M., Cesarsky C.J., Elbaz D., Pelló R., Soucail G., Vigroux L., 1998, A&A, 334, L21
Metcalfe L., Altieri B., McBreen B., Kneib J.-P., Delaney M. et al., 1999, ISO Paris conf. proc., in press
Metcalfe L. et al., 1999b, in preparation.
Oliver S., Goldschmidt P., Franceschini A. et al., 1997, MNRAS, 289, 471
Pelló R., LeBorgne J.F., Soucail G., Mellier Y., Sanahuja B., 1991, ApJ, 366, 405
Rowan-Robinson M., Mann R., Oliver S. et al., 1997, MNRAS 289, 490
Starck J.-L. et al., 1997, in *Extragalactic Astronomy in the Infrared*, Edt Frontieres, G. Mamon
Smail I., Ivison R.J., Blain A.W., 1997, ApJ, 1997, 490, L5
Soucail G. et al., 1999, A&A letter in press, astro-ph/9901123
Stanev T. and Franceschini A., 1998, ApJ, 494, L159
Steidel C.S., Giavalisco M, Dickinson M., 1996, AJ 112, 352
Taniguchi Y., Cowie L., Sato Y. et al., 1997, A&A, 328, L9